

## Communication: Coherences observed *in vivo* in photosynthetic bacteria using two-dimensional electronic spectroscopy

Peter D. Dahlberg,<sup>1</sup> Graham J. Norris,<sup>2</sup> Cheng Wang,<sup>2</sup> Subha Viswanathan,<sup>2</sup> Ved P. Singh,<sup>2</sup> and Gregory S. Engel<sup>2,a)</sup>

<sup>1</sup>Graduate Program in the Biophysical Sciences, Institute for Biophysical Dynamics, and The James Franck Institute, The University of Chicago, Chicago, Illinois 60637, USA

<sup>2</sup>Department of Chemistry, Institute for Biophysical Dynamics, and The James Franck Institute, The University of Chicago, Chicago, Illinois 60637, USA

(Received 10 July 2015; accepted 19 August 2015; published online 9 September 2015)

Energy transfer through large disordered antenna networks in photosynthetic organisms can occur with a quantum efficiency of nearly 100%. This energy transfer is facilitated by the electronic structure of the photosynthetic antennae as well as interactions between electronic states and the surrounding environment. Coherences in time-domain spectroscopy provide a fine probe of how a system interacts with its surroundings. In two-dimensional electronic spectroscopy, coherences can appear on both the ground and excited state surfaces revealing detailed information regarding electronic structure, system-bath coupling, energy transfer, and energetic coupling in complex chemical systems. Numerous studies have revealed coherences in isolated photosynthetic pigment-protein complexes, but these coherences have not been observed *in vivo* due to the small amplitude of these signals and the intense scatter from whole cells. Here, we present data acquired using ultrafast video-acquisition gradient-assisted photon echo spectroscopy to observe quantum beating signals from coherences *in vivo*. Experiments were conducted on isolated light harvesting complex II (LH2) from *Rhodobacter sphaeroides*, whole cells of *R. sphaeroides*, and whole cells of *R. sphaeroides* grown in 30% deuterated media. A vibronic coherence was observed following laser excitation at ambient temperature between the B850 and the B850\* states of LH2 in each of the 3 samples with a lifetime of ~40-60 fs. © 2015 AIP Publishing LLC. [<http://dx.doi.org/10.1063/1.4930539>]

Photosynthetic organisms utilize large arrays of light harvesting antenna to maximize their absorption cross section and to improve their solar harvesting capabilities. The very first events after absorption of a photon in photosynthesis involve the transfer of excitation through these large antenna networks to the reaction center where the bound electron-hole pair is separated. The energy transfer process through the antenna network can be nearly 100% quantum efficient.<sup>1,2</sup> Given the noisy, disordered environment within membranes of living cells, this high quantum efficiency is surprising. Many theories and experiments have been developed and performed to understand how photosynthetic organisms obtain such quantum-efficient energy transfer.<sup>3,4</sup> In 2007, two-dimensional electronic spectroscopy (2DES) showed long-lived coherences within the Fenna-Mathews-Olson (FMO) complex, a pigment-protein complex found in green sulfur bacteria; these coherences were attributed to excited states.<sup>5</sup> Similar work was conducted on other pigment-protein complexes, finding that they too exhibited long-lived coherences.<sup>6-11</sup> Several models have suggested that long-lived electronic coherences may help to explain the high quantum efficiencies observed in photosynthesis.<sup>3,4,12</sup> Further experiments show that these long-lived coherences persist at room temperature, but with reduced lifetimes.<sup>9,13,65</sup> Currently, the nature of these coherences, either vibrational, electronic, or some mixture of vibrational

and electronic (vibronic), is under debate.<sup>14-16</sup> Recent works have classified many of these coherences as vibronic, with several recent publications providing experimental evidence for vibronic coherences as well as several models outlining their importance in energy transfer and possibly charge separation.<sup>10,11,17-20</sup> It is not the aim of this work to assign the nature of these coherences or to provide evidence for a given model, rather this work addresses the debate of the biological significance of these coherences by observing them *in vivo*—a necessary prerequisite for biological significance.

In the discussion surrounding the biological significance of these coherences, it has always been assumed that the coherences observed *in vitro* also occur *in vivo*. While it would be surprising if these coherences did not occur *in vivo*, it is necessary to confirm this assumption. Beyond mere existence, there are numerous reasons why the coherences may be different *in vivo* and *in vitro*. The coherences could differ in spectral location due to coupling to the intact photosynthetic unit as well as the presence of a large electric field (~10<sup>7</sup> V/m) spanning the photosynthetic membrane known to cause electrochromic shifts.<sup>21</sup> The coherences may also differ in lifetime due to inhomogeneity of the biological environment. Coherence lifetime measurements in two-dimensional spectroscopy experiments are sensitive to both single molecule decoherence and ensemble dephasing.<sup>22</sup> Both effects are due to system-bath interactions and it is unclear how the complex and crowded environment *in vivo* will affect observed lifetimes in these complexes. Crowding *in vivo*

<sup>a)</sup> Author to whom correspondence should be addressed. Electronic mail: [gsengel@uchicago.edu](mailto:gsengel@uchicago.edu)

could lead to increased disorder in system bath interactions and therefore shorter lifetimes, or it could be that the higher viscosity of the lipid bilayer reduces stochastic system-bath interactions and would increase coherent lifetimes *in vivo*. It is also possible that the environments are similar enough to produce no appreciable changes. These competing effects of unknown magnitudes make it difficult to predict changes to the lifetimes of coherences between *in vitro* and *in vivo* preparations, and it is also likely that different systems will respond differently to the changes in environment.

The technique of 2DES is well suited for the observation of coherences in biological systems. However, the interferometry can be frustrated by highly scattering systems like whole cells. Recent developments have focused both on overcoming scatter and decreasing experiment time to allow for triplicated results.<sup>23–26</sup> Here, we surmount both issues—intense scattered light and the quantification of errors—using Ultrafast Video-Acquisition Gradient-Assisted Photon-Echo Spectroscopy (UVA-GRAPES) to observe coherences in the pigment-protein complex, light harvesting complex II (LH2), in whole cells of the purple bacterium, *Rhodospira rubra*.

The antenna in *R. rubra* consists of two pigment-protein complexes, light harvesting complex I (LH1) and light harvesting complex II (LH2).<sup>27</sup> LH1 and LH2 are embedded in invaginations of the cell membrane known as chromatophores. *In vivo*, LH1 is a core antenna complex that dimerizes and encircles the reaction centers.<sup>28–30</sup> LH2 complexes are peripheral to the LH1 dimers, transferring energy to LH1 on a time scale of 5–7 ps.<sup>31</sup> LH1 in turn transfers the excitation to the special pair in the reaction center on a time scale of 35 ps.<sup>31</sup>

LH2 contains two rings of bacteriochlorophyll *a* known as B800 and B850 which predominately absorb at 800 nm and 850 nm, respectively, see Figure 1.<sup>32</sup> The B850 ring has a higher-lying set of excited states known as the B850\* states that absorb near 800 nm (~770–815 nm), overlapping with the B800 band.<sup>33,34</sup> The B800 ring is composed of nine weakly coupled ( $J \approx 20 \text{ cm}^{-1}$ ) bacteriochlorophyll *a*, whereas the B850 ring is composed of eighteen strongly coupled ( $J \approx 300 \text{ cm}^{-1}$ ) bacteriochlorophyll *a*.<sup>31</sup> Both rings are red-shifted compared to free bacteriochlorophyll *a*; for B800, this shift is due to protein–bath interactions,<sup>35</sup> while for B850, the shift arises primarily from chromophore–chromophore

interactions.<sup>31</sup> The two rings are weakly coupled to each other ( $J \approx 20\text{--}50 \text{ cm}^{-1}$ ).<sup>31</sup>

Energy transfer from LH2 to LH1 occurs from the B850 states.<sup>31,36</sup> Several energy transfer pathways exist connecting the higher-lying excited states in LH2 to the low-lying B850 states:  $B800 \rightarrow B850^* \rightarrow B850$ ,  $B800 \rightarrow B850$ , and  $B850^* \rightarrow B800 \rightarrow B850$ .<sup>34,37</sup> The time scales for energy transfer along these pathways have been modeled using Redfield theory and experimentally determined.<sup>38–43</sup> Energy transfer from B800 to B850\* occurs with a lifetime of ~500–800 fs and from B800 to B850 with a lifetime of ~700–1000 fs. The back-transfer from B850\* to B800 is slower (>250 fs) than the transfer from B850\* to B850 (~60–200 fs). Comparable rates of transfer from B800 to B850\* and from B800 to B850 suggest that comparable amounts of energy are transferred over both pathways. Thus, the B850\* states play an important role in directing energy flow from B800 to B850 and thereby to LH1.<sup>34</sup> Coherent mechanisms may play a crucial role in the energy transfer from B850\* to B850. Room-temperature coherences between states near 800 nm and states near 850 nm have been observed with a lifetime of ~50–100 fs and were originally attributed to electronic coherence between B800 and B850 as well as to electronic coherence between B850\* and B850.<sup>44,45</sup> Recent work on a mutant strain of *R. rubra* lacking the B800 chromophore ring found similar coherences, suggesting that the coherence is not between B800 and B850, but between B850\* and B850.<sup>46</sup> Further analysis in the same work using a coherence specific pulse sequence was able to quantify the mixing of vibrational and electronic states in the coherence between B850 and B850\* and found a mixing angle of ~15° and classified the coherence as vibronic.<sup>46</sup>

2DES is ideally suited for the study of the initial energy transfer events and coherent processes in photosynthesis. This ultrafast technique can measure energy transfer dynamics on time scales from tens of femtoseconds to hundreds of picoseconds. Furthermore, the technique separates crowded linear spectra into two-dimensional correlation maps.<sup>47–53</sup> The UVA-GRAPES instrument, used to acquire the 2DES signal in this study, has been described elsewhere.<sup>23</sup> Briefly, the output of a 5 kHz regenerative amplifier (coherent Legend Elite) is focused into a 2.25 m tube of argon at ~1–2 psi above atmospheric pressure in order to produce a white-light continuum through filamentation. The resulting pulse is shaped and compressed to 15 fs FWHM centered at ~790 nm with ~120 nm of bandwidth using a multiphoton intrapulse interference phase scan compressor (Biophotonics Solutions, Inc.). Figure 1 shows a normalized excitation spectrum as well as a normalized absorbance spectrum of LH2. Following compression, the pulse is separated into the four-pulse sequence required for 2DES. The powers for pulses 1–3 are attenuated to 500 nJ each at the sample. The UVA-GRAPES apparatus encodes the coherence time, time between pulses 1 and 2, spatially across the sample and necessitates focusing to a line (~6 mm by ~60 μm) rather than a spot at the sample. The resulting energy flux is only 137 μJ/cm<sup>2</sup> per pulse (~5.5 × 10<sup>14</sup> photons/cm<sup>2</sup> per pulse), comparable to numerous other studies and below the threshold for multi-exciton effects.<sup>40,42,45,54</sup> The local oscillator (LO) is attenuated an additional two orders of magnitude and adjusted

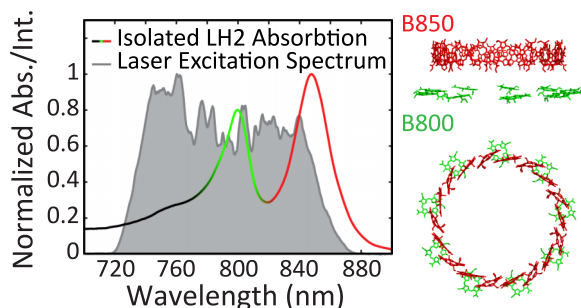


FIG. 1. The normalized absorption spectrum of isolated LH2 is plotted (black-green-red solid gradient line) to emphasize the correlation between the absorption features and the two rings of bacteriochlorophyll *a* shown in profile to the right. The laser excitation spectra used to perform 2DES experiments are shown in shaded gray and are the result of filamentation in argon gas and pulse shaping with a spatial light modulator.

to arrive  $\sim 3$  ps ahead of the other pulses to avoid pump-probe artifacts. Encoding the coherence time delay spatially across the sample allows for the completion of a 2DES experiment with just a single scan of the waiting time, time between pulses 2 and 3.<sup>55</sup> Using a high-speed camera as a detector, the UVA-GRAPES instrument can record a 2DES spectrum on every laser shot, reducing the data acquisition time to just a few seconds.<sup>23</sup> The high-speed acquisition permits fine sampling of the waiting time, approximately every 600 as. Numerous scatter contributions oscillate in the waiting time domain at the optical period and this fine sampling permits their removal in the waiting time frequency domain without distorting the dynamics of the 2DES signal.<sup>23</sup> This approach allows the UVA-GRAPES instrument to observe 2DES signals from samples that scatter light intensely, such as the whole cells of *R. sphaeroides* presented in this manuscript.

*Rhodobacter sphaeroides* was cultured aerobically and in the dark at 28 °C. Cells were cultured with either H<sub>2</sub>O or 30% D<sub>2</sub>O. The cells grown in 30% D<sub>2</sub>O were intended to help isolate electronic or vibronic coherences from purely vibrational coherences.<sup>56,66</sup> Cells for analysis were centrifuged at 6000 rpm (rotor JLA 8.1) and diluted in a small volume of their supernatant, maintaining D<sub>2</sub>O concentrations, to achieve an OD<sub>800</sub> of  $\sim 0.07$  in a 200  $\mu\text{m}$  quartz flow cell (Starna Cells, Inc.). For isolated LH2 experiments, the complex was isolated from the H<sub>2</sub>O cells according to the protocol outlined by Frank *et al.*<sup>57</sup> The cells were lysed via sonication and the large cell fragments were separated by slow centrifugation (12 000 rpm Beckman Coulter, Inc. rotor JA 30.50). The supernatant was ultra-centrifuged (50 000 rpm Beckman Coulter, Inc. rotor <sup>60</sup>Ti). The pellet was re-suspended and run through a DEAE-Sephacel column twice and eluted with 500-600 mM NaCl. The sample was buffer-exchanged into 20 mM Tris, 0.06% LDAO at pH 7.5, and concentrated to an OD<sub>800</sub> of  $\sim 0.22$  in the flow cell described above. The absorption spectra of the cells grown in H<sub>2</sub>O and D<sub>2</sub>O as well as the isolated LH2 are shown in Figure S1 in the supplementary material<sup>64</sup> with Raleigh scatter subtracted.

Figure 2 shows the absolute value 2DES rephasing spectra for isolated LH2, cells grown in the D<sub>2</sub>O media, and cells grown in the H<sub>2</sub>O media at a waiting time of 50 fs. Within error, the three plots are consistent and all three show dynamics

and features similar to previously published LH2 spectra. The rephasing spectra can also be phased in a manner described by Singh *et al.* using separately acquired pump-probe data, see Figure S2 in the supplementary material.<sup>58,64</sup> In the phased data, we see  $\sim 100$  fs decay of the 850 nm diagonal region. This decay has previously been attributed to the stochastic hopping of the exciton around the B850 ring as well as relaxation to lower energy states within the B850 band.<sup>34,45,59,60</sup> The growth of a cross peak between the B800 and B850 nm states is on the order of  $\sim 700$  fs, and a corresponding decay of the B800 states is also observed and is indicative of energy transfer from B800 to B850. In addition to these population transfers at early waiting times, coherent oscillations in the upper and lower cross-peaks in the region between the B800 and B850 bands are also observed. Due to slight uncertainties in the phasing and the possibility of improper phasing introducing modulations that can be mistaken as coherences, all analyses relating to the coherences are done with the absolute value data.

Subtracting a bi-exponential from the waiting time domain and Fourier transforming, the residual from 0 to 200 fs clarifies the coherent oscillations between B850\* and B850 in the absolute value data. The center of the B850\* peak occurs at  $\sim 795$  nm, so a coherence between B850 and B850\* should appear with a beat frequency of approximately 850 cm<sup>-1</sup> (the energy difference between the center of the two states). Due to the short waiting time period considered, the frequency domain necessarily has widely spaced frequency points, with the two closest points being 830 and 1000 cm<sup>-1</sup>. The bottom row of Figure 3 displays the separately normalized power spectra for each pixel at 830 cm<sup>-1</sup>, the same analysis is shown in Figure S3<sup>64</sup> for a waiting time frequency of 1000 cm<sup>-1</sup>. The full map of LH2 shows peaks located at both the upper and the lower cross peaks between B850 and B850\*. The middle row of Figure 3 details the upper cross peak and highlights the similarity in location and intensity of oscillations between all three samples. The top row of Figure 3 depicts the phase of the oscillations over the same region as detailed in the middle row. All three samples show the same phase and phase roll across the diagonal of the peak. A phase roll is characteristic of both electronic and vibrational coherences.<sup>61-63</sup> Figure 4 shows waiting time traces from the upper cross peak for the isolated LH2, D<sub>2</sub>O cells, and H<sub>2</sub>O cells, again displaying similarities in phase

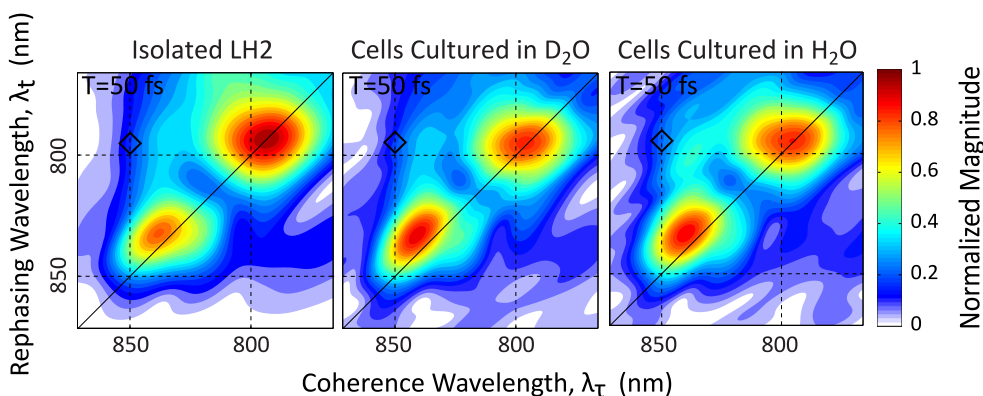


FIG. 2. Absolute value 2DES spectra showing the magnitude of the rephasing signal at  $T = 50$  fs are shown for isolated LH2 (left), cells grown in 30% D<sub>2</sub>O media (middle), and cells grown in standard H<sub>2</sub>O media (right). For each data set, the magnitude was separately normalized to the maximum of the entire waiting time scan. The black diamond indicates the location of the waiting time traces shown in Figure 4.

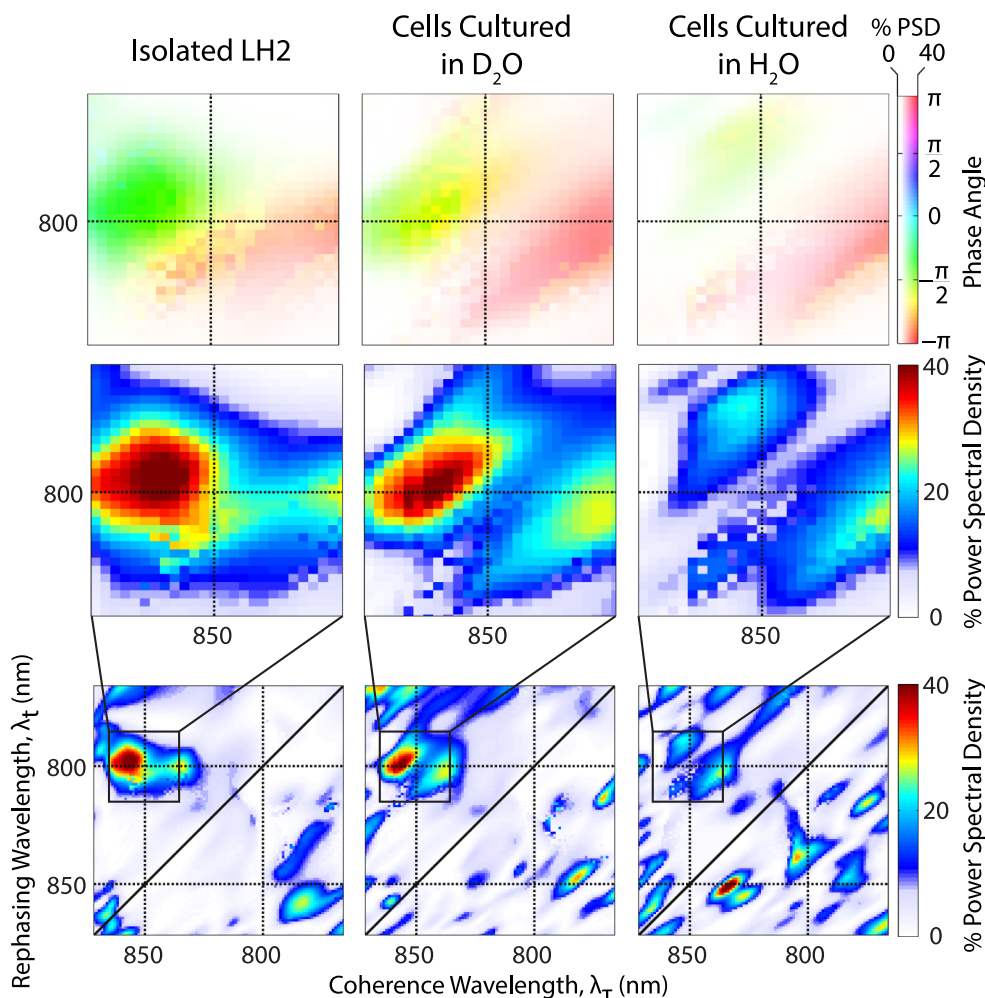


FIG. 3. Bottom row: Power spectral density at  $830\text{ cm}^{-1}$  represented as a percentage of the normalized, integrated power spectrum from the absolute value data. Middle row: Detail of the power spectrum at the 800-850 nm upper cross peak boxed in the bottom row. Top row: Phase of the  $830\text{ cm}^{-1}$  oscillations over the same region, with the saturation determined by the power spectral density from the middle row.

and amplitude between samples. The  $1\sigma$  standard error on the mean is displayed as the shaded region and is calculated from sixteen separate scans performed on each sample. The red lines indicate the fit of an exponentially damped sine wave to the residual of the bi-exponential fit. A regression was performed for each pixel within the region shown in the top and middle rows of Figure 3. The resulting lifetimes are provided in Figure S4 in the supplementary material<sup>64</sup> and are found to be  $\sim 40$ - $60$  fs, comparable to coherences previously observed in isolated LH2. This short lifetime is reflected in the waiting time frequency domain by a broad peak in the power spectra, which can be seen in Figure S5.<sup>64</sup> The distinct differences in amplitude and lifetime between the pure vibrational coherences and the vibronic coherence can be seen in Figures S6 and S7.<sup>64</sup>

Vibronic coherence between B850 and B850\*, while lasting less than 100 fs, has a similar lifetime to that of energy transfer between these states,  $\sim 60$ - $200$  fs. The biological significance of this coherence is unclear, but due to the B850\* states playing an intermediate role in the energy transfer pathways between the B800 and B850 states,<sup>34</sup> this coherence could play a significant role in improving the efficiency of solar light harvesting in *R. sphaeroides*. Observation of this coherence *in vivo* and its similarity to the coherence observed

*in vitro* supports the assumption that coherences are robust to the environmental changes between the native photosynthetic membrane and detergent micelles. It is possible, however, that this coherence is uniquely similar *in vitro* and *in vivo* because the coherence is supported by different excited states

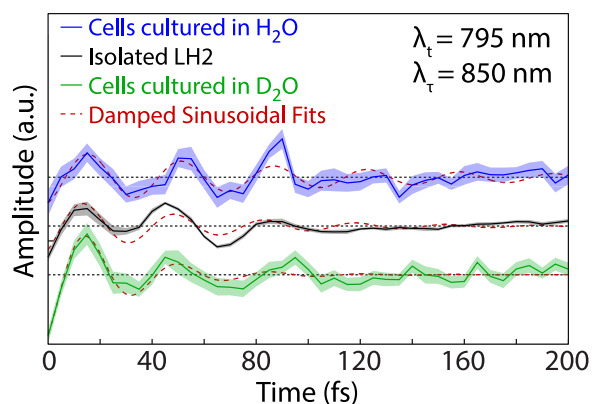


FIG. 4. Waiting time traces from the B850-B850\* upper cross peak ( $\lambda_t = 795\text{ nm}$ ,  $\lambda_\tau = 850\text{ nm}$ ) for isolated LH2, D<sub>2</sub>O cells, and H<sub>2</sub>O cells. The shaded region is the standard error from 16 separate scans for each data set. The red lines indicate a fit to an exponentially damped sine wave.

on the same ring of chromophores, making it more robust to changes in environment. Future work must be done to determine whether other photosynthetic coherences exhibit this robustness and whether these coherences are dependent upon growth conditions. Further work will also examine whether coherences change in response to external stimuli such as intense light or the addition of oxygen, which are known to induce photoprotective mechanisms.

The authors would like to thank NSF MRSEC (Grant No. DMR 14-20709), the Keck Foundation, AFOSR (Grant No. FA9550-09-1-0117), the DARPA QuBE program (No. N66001-10-1-4060), and DTRA (No. HDTRA1-10-1-0091) for supporting this work. P.D.D. acknowledges support from the NSF GRFP. P.D.D. was supported by the Graduate Program in Biophysical Sciences at the University of Chicago (NIH Grant No. T32 Eb009412).

- <sup>1</sup>C. A. Wraight and R. K. Clayton, *Biochim. Biophys. Acta, Bioenerg.* **333**, 246 (1974).
- <sup>2</sup>R. K. Chain and D. I. Arnon, *Proc. Natl. Acad. Sci. U. S. A.* **74**, 3377 (1977).
- <sup>3</sup>P. Rebentrost, M. Mohseni, I. Kassal, S. Lloyd, and A. Aspuru-Guzik, *New J. Phys.* **11**, 033003 (2009).
- <sup>4</sup>M. Mohseni, P. Rebentrost, S. Lloyd, and A. Aspuru-Guzik, *J. Chem. Phys.* **129**, 174106 (2008).
- <sup>5</sup>G. S. Engel, T. R. Calhoun, E. L. Read, T. K. Ahn, T. Mancal, Y. C. Cheng, R. E. Blankenship, and G. R. Fleming, *Nature* **446**, 782 (2007).
- <sup>6</sup>H. Lee, Y. C. Cheng, and G. R. Fleming, *Science* **316**, 1462 (2007).
- <sup>7</sup>G. S. Schlau-Cohen, E. De Re, R. J. Cogdell, and G. R. Fleming, *J. Phys. Chem. Lett.* **3**, 2487 (2012).
- <sup>8</sup>G. S. Schlau-Cohen, A. Ishizaki, T. R. Calhoun, N. S. Ginsberg, M. Ballottari, R. Bassi, and G. R. Fleming, *Nat. Chem.* **4**, 389 (2012).
- <sup>9</sup>E. Collini, C. Y. Wong, K. E. Wilk, P. M. Curmi, P. Brumer, and G. D. Scholes, *Nature* **463**, 644 (2010).
- <sup>10</sup>F. D. Fuller, J. Pan, A. Gelzinis, V. Butkus, S. S. Senlik, D. E. Wilcox, C. F. Yocum, L. Valkunas, D. Abramavicius, and J. P. Ogilvie, *Nat. Chem.* **6**, 706 (2014).
- <sup>11</sup>E. Romero, R. Augulis, V. I. Novoderezhkin, M. Ferretti, J. Thieme, D. Zigmantas, and R. van Grondelle, *Nat. Phys.* **10**, 677 (2014).
- <sup>12</sup>A. Ishizaki and G. R. Fleming, *Proc. Natl. Acad. Sci. U. S. A.* **106**, 17255 (2009).
- <sup>13</sup>G. Panitchayangkoon, D. Hayes, K. A. Fransted, J. R. Caram, E. Harel, J. Wen, R. E. Blankenship, and G. S. Engel, *Proc. Natl. Acad. Sci. U. S. A.* **107**, 12766 (2010).
- <sup>14</sup>V. Tiwari, W. K. Peters, and D. M. Jonas, *Proc. Natl. Acad. Sci. U. S. A.* **110**, 1203 (2013).
- <sup>15</sup>K. A. Fransted, J. R. Caram, D. Hayes, and G. S. Engel, *J. Chem. Phys.* **137**, 125101 (2012).
- <sup>16</sup>N. Christensson, F. Milota, J. Hauer, J. Sperling, O. Bixner, A. Nemeth, and H. F. Kauffmann, *J. Phys. Chem. B* **115**, 5383 (2011).
- <sup>17</sup>J. M. Womick and A. M. Moran, *J. Phys. Chem. B* **115**, 1347 (2011).
- <sup>18</sup>A. Chenu and G. D. Scholes, *Annu. Rev. Phys. Chem.* **66**, 69 (2015).
- <sup>19</sup>V. Tiwari, W. K. Peters, and D. M. Jonas, *Nat. Chem.* **6**, 173 (2014).
- <sup>20</sup>A. Chenu, N. Christensson, H. F. Kauffmann, and T. Mancal, *Sci. Rep.* **3**, 2029 (2013).
- <sup>21</sup>W. Junge, *Annu. Rev. Plant Physiol.* **28**, 503 (1977).
- <sup>22</sup>K. M. Pelzer, G. B. Griffin, S. K. Gray, and G. S. Engel, *J. Chem. Phys.* **136**, 164508 (2012).
- <sup>23</sup>P. D. Dahlberg, A. F. Fidler, J. R. Caram, P. D. Long, and G. S. Engel, *J. Phys. Chem. Lett.* **4**, 3636 (2013).
- <sup>24</sup>J. Dostal, T. Mancal, R. Augulis, F. Vacha, J. Psencik, and D. Zigmantas, *J. Am. Chem. Soc.* **134**, 11611 (2012).
- <sup>25</sup>R. Augulis and D. Zigmantas, *Opt. Express* **19**, 13126 (2011).
- <sup>26</sup>D. G. Osborne and K. J. Kubarych, *J. Phys. Chem. A* **117**, 5891 (2013).
- <sup>27</sup>J. Aagaard and W. R. Siström, *Photochem. Photobiol.* **15**, 209 (1972).
- <sup>28</sup>C. Jungas, J. L. Ranck, J. L. Rigaud, P. Joliot, and A. Vermeglio, *EMBO J.* **18**, 534 (1999).
- <sup>29</sup>S. Bahatyrova, R. N. Frese, C. A. Siebert, J. D. Olsen, K. O. van der Werf, R. van Grondelle, R. A. Niederman, P. A. Bullough, C. Otto, and C. N. Hunter, *Nature* **430**, 1058 (2004).
- <sup>30</sup>C. A. Siebert, P. Qian, D. Fotiadis, A. Engel, C. N. Hunter, and P. A. Bullough, *EMBO J.* **23**, 690 (2004).
- <sup>31</sup>V. Sundström, T. Pullerits, and R. van Grondelle, *J. Phys. Chem. B* **103**, 2327 (1999).
- <sup>32</sup>G. McDermott, S. M. Prince, A. A. Freer, A. M. Hawthornthwaitelawless, M. Z. Papiz, R. J. Cogdell, and N. W. Isaacs, *Nature* **374**, 517 (1995).
- <sup>33</sup>M. H. Koolhaus, R. N. Frese, G. J. Fowler, T. S. Bibby, S. Georgakopoulou, G. van der Zwan, C. N. Hunter, and R. van Grondelle, *Biochemistry* **37**, 4693 (1998).
- <sup>34</sup>V. Novoderezhkin, M. Wendling, and R. van Grondelle, *J. Phys. Chem. B* **107**, 11534 (2003).
- <sup>35</sup>G. J. Fowler, S. Hess, T. Pullerits, V. Sundstrom, and C. N. Hunter, *Biochemistry* **36**, 11282 (1997).
- <sup>36</sup>G. R. Fleming and R. van Grondelle, *Curr. Opin. Struct. Biol.* **7**, 738 (1997).
- <sup>37</sup>A. F. Fidler, V. P. Singh, P. D. Long, P. D. Dahlberg, and G. S. Engel, *J. Chem. Phys.* **139**, 155101 (2013).
- <sup>38</sup>J. K. Trautman, A. P. Shreve, C. A. Violette, H. A. Frank, T. G. Owens, and A. C. Albrecht, *Proc. Natl. Acad. Sci. U. S. A.* **87**, 215 (1990).
- <sup>39</sup>H. van der Laan, T. Schmidt, R. W. Visschers, K. J. Visscher, R. van Grondelle, and S. Völker, *Chem. Phys. Lett.* **170**, 231 (1990).
- <sup>40</sup>R. Monshouwer, I. O. Dezarate, F. Vanmourik, and R. Vangrondelle, *Chem. Phys. Lett.* **246**, 341 (1995).
- <sup>41</sup>S. Hess, E. Akesson, R. J. Cogdell, T. Pullerits, and V. Sundstrom, *Biophys. J.* **69**, 2211 (1995).
- <sup>42</sup>T. H. Joo, Y. W. Jia, J. Y. Yu, D. M. Jonas, and G. R. Fleming, *J. Phys. Chem.* **100**, 2399 (1996).
- <sup>43</sup>J. L. Herek, N. J. Fraser, T. Pullerits, P. Martinsson, T. Polivka, H. Scheer, R. J. Cogdell, and V. Sundstrom, *Biophys. J.* **78**, 2590 (2000).
- <sup>44</sup>E. Harel and G. S. Engel, *Proc. Natl. Acad. Sci. U. S. A.* **109**, 706 (2012).
- <sup>45</sup>A. F. Fidler, V. P. Singh, P. D. Long, P. D. Dahlberg, and G. S. Engel, *J. Phys. Chem. Lett.* **4**, 1404 (2013).
- <sup>46</sup>V. P. Singh, M. Westberg, C. Wang, P. D. Dahlberg, T. Gellen, A. T. Gardiner, R. J. Cogdell, and G. S. Engel, *J. Chem. Phys.* **142**, 212446 (2015).
- <sup>47</sup>D. M. Jonas, *Annu. Rev. Phys. Chem.* **54**, 425 (2003).
- <sup>48</sup>S. Mukamel, *Principles of Nonlinear Optical Spectroscopy*, Oxford Series in Optical and Imaging Sciences Vol. 6 (Oxford University Press, New York, Oxford, 1995).
- <sup>49</sup>J. D. Hybl, A. A. Ferro, and D. M. Jonas, *J. Chem. Phys.* **115**, 6606 (2001).
- <sup>50</sup>M. Cho, H. M. Vaswani, T. Brixner, J. Stenger, and G. R. Fleming, *J. Phys. Chem. B* **109**, 10542 (2005).
- <sup>51</sup>T. Brixner, T. Mancal, I. V. Stiopkin, and G. R. Fleming, *J. Chem. Phys.* **121**, 4221 (2004).
- <sup>52</sup>M. L. Cowan, J. P. Ogilvie, and R. J. D. Miller, *Chem. Phys. Lett.* **386**, 184 (2004).
- <sup>53</sup>J. D. Hybl, A. W. Albrecht, S. M. G. Faeder, and D. M. Jonas, *Chem. Phys. Lett.* **297**, 307 (1998).
- <sup>54</sup>E. Harel, A. F. Fidler, and G. S. Engel, *J. Phys. Chem. A* **115**, 3787 (2011).
- <sup>55</sup>E. Harel, P. D. Long, and G. S. Engel, *Opt. Lett.* **36**, 1665 (2011).
- <sup>56</sup>D. Hayes, J. Wen, G. Panitchayangkoon, R. E. Blankenship, and G. S. Engel, *Faraday Discuss.* **150**, 459 (2011).
- <sup>57</sup>H. A. Frank, B. W. Chadwick, J. J. Oh, D. Gust, T. A. Moore, P. A. Liddell, A. L. Moore, L. R. Makings, and R. J. Cogdell, *Biochim. Biophys. Acta, Bioenerg.* **892**, 253 (1987).
- <sup>58</sup>V. P. Singh, A. F. Fidler, B. S. Rolczynski, and G. S. Engel, *J. Chem. Phys.* **139**, 084201 (2013).
- <sup>59</sup>A. F. Fidler, V. P. Singh, P. D. Long, P. D. Dahlberg, and G. S. Engel, *Nat. Commun.* **5**, 3286 (2014).
- <sup>60</sup>R. Jimenez, F. vanMourik, J. Y. Yu, and G. R. Fleming, *J. Phys. Chem. B* **101**, 7350 (1997).
- <sup>61</sup>V. Butkus, D. Zigmantas, L. Valkunas, and D. Abramavicius, *Chem. Phys. Lett.* **545**, 40 (2012).
- <sup>62</sup>G. Panitchayangkoon, D. V. Voronine, D. Abramavicius, J. R. Caram, N. H. Lewis, S. Mukamel, and G. S. Engel, *Proc. Natl. Acad. Sci. U. S. A.* **108**, 20908 (2011).
- <sup>63</sup>J. Seibt and T. Pullerits, *J. Chem. Phys.* **141**, 114106 (2014).
- <sup>64</sup>See supplementary material at <http://dx.doi.org/10.1063/1.4930539> for figures displaying additional spectra as well as a brief discussion of regression and noise.
- <sup>65</sup>The term “long-lived” is ambiguous. In this manuscript, a long-lived coherence is one that persists on the same time scale as that of energy transfer in the system under study.
- <sup>66</sup>Room temperature dephasing rates prevent attribution of the coherences by isotopic substitution, but we chose to present the data because they show the reproducibility of the dynamics across samples.